NASA TECHNICAL NOTE

NASA TN D-3949

NASA TN D-3949

HIGH-VOLTAGE CHARACTERISTICS OF A LARGE-GAP COAXIAL-CYLINDER ELECTRODE

by Kenneth F. Koral

Lewis Research Center

Cleveland, Ohio

NATIONAL AERONAUTICS AND SPACE ADMINISTRATION • WASHINGTON, D. C. • MAY 1967

HIGH-VOLTAGE CHARACTERISTICS OF A LARGE-GAP COAXIAL-CYLINDER ELECTRODE

By Kenneth F. Koral

Lewis Research Center
Cleveland, Ohio

NATIONAL AERONAUTICS AND SPACE ADMINISTRATION

For sale by the Clearinghouse for Federal Scientific and Technical Information
Springfield, Virginia 22151 – CFSTI price $3.00

HIGH-VOLTAGE CHARACTERISTICS OF A LARGE-GAP COAXIAL-CYLINDER ELECTRODE

by Kenneth F. Koral

Lewis Research Center

SUMMARY

Measurements of prebreakdown currents, conditioning rates, and ultimate voltage capability were made for a 30-centimeter-gap, concentric-cylinder configuration in a continuously pumped vacuum environment. Both micropulsing and continuous currents flowed across the vacuum gaps at voltages above a threshold value. A linear dependence of threshold voltage on the total charge that had traversed the gap was found for a certain range of conditions. The ultimate vacuum-gap voltage with a positive inner cylinder was 395 kilovolts at 10^{-7} torr and greater than 600 kilovolts at an optimum background gas pressure (approximately 2×10^{-4} torr). Tests showed that a 44-centimeter-long polycarbonate insulator with negative junction shielding operated well at voltages up to 600 kilovolts. Experimental results did not correlate well with either the field-emission or the particle-exchange theory of prebreakdown conduction.

INTRODUCTION

Prebreakdown leakage currents (i.e., currents not associated with a voltage collapse) and ultimate voltage capability of solid and vacuum insulation are critically important in a number of applications, for example, in the direct nuclear electrogenerator. Such an electrogenerator consists of a radioisotope deposited on a metal electrode insulated from ground by a solid insulator. A second electrode at ground potential faces the first across a vacuum gap. Passage of charged decay particles across the vacuum gap builds up a high voltage on the first electrode. This voltage can then be used to power a high-impedance device (ref. 1). According to the theoretical calculations of reference 2, a cylindrical radioisotope electrogenerator using beta-emitting cerium requires a total voltage of approximately 600 kilovolts to operate at maximum efficiency. It has been observed experimentally, however, in tests with an alpha-cell direct-conversion genera-

tor, that vacuum-gap leakage currents may present operational problems that limit voltage buildup (ref. 3).

Past investigations on the threshold voltage and nature of prebreakdown leakage currents involve mainly small (1-cm) vacuum gaps (refs. 4 to 6). Reference 6 reports that the prebreakdown currents decrease in time, a phenomenon which is called conditioning or forming of the electrodes. Detailed information on the rate of conditioning, however, does not exist in the literature. For the ultimate voltage capability for a large vacuum gap, data are available mainly for plane electrodes (ref. 7), and no measurements have been made on cylindrical electrodes with gaps larger than 1 centimeter.

Investigations of the voltage capability of solid insulation are also typically limited to dimensions of the order of 1 centimeter (refs. 8 and 9). The breakdown current almost always occurs along the insulator surface and is attributed to field intensification at the triple junction of insulator, negative electrode, and vacuum (ref. 9). Placing metal shields around this junction to reduce the macroscopic field is reported to increase the standoff voltage (ref. 10).

This report contains high-voltage measurements on a large-gap cylindrical electrode configuration. Data are also presented on large-dimension, organic insulation that is shielded at the negative junction. No radioisotopes were utilized; voltages were applied by a power supply outside the vacuum system. A preliminary report of the data appears in reference 11.

APPARATUS

The configuration that was investigated is shown in figure 1(a). The inner cylinder was 0.279 meter in diameter and 1.15 meters in length. The outer cylinder was 0.864 meter in diameter and 1.84 meters in length. Both solid and screen outer cylinders were used. Top and bottom end caps were electrically isolated and placed as shown. All electrodes were 304 stainless steel except the negative junction shield, which was aluminum. Large scratches were removed from the electrodes, which were otherwise unpolished. They were cleaned with acetone followed by alcohol before each test.

The inner cylinder was separated from ground by a 0.445-meter-long hollow-tube polycarbonate insulator. The top of the tube was covered by a metal cap and the bottom was encircled by a metal collar. Both were sealed to the tube with an epoxy cement. In order to supply voltage to the inner cylinder, a 5.1-centimeter-diameter high-voltage cable, with ground shield removed, was inserted through the hollow insulator and connected to the bottom plate of the inner cylinder.

Voltage for the experiment was supplied by a 600-kilovolt, 20-milliampere power supply. A 1.57-gigaohm, surge-limiting resistance was placed in series with the supply.

Capacitance of the electrode configuration was 90 picofarads. The high-voltage cable between the electrode configuration and the surge-limiting resistance had a capacitance of 750 picofarads. Applied voltage was measured at the power supply by a voltage divider and a millivoltmeter, and a correction was made for the losses across the surge-limiting resistance. Individual microameters and recording oscillograph galvanometers were attached to each of the isolated ground electrodes to determine both the nature and location of prebreakdown currents (fig. 1(b)). The product of current and time for any given period was monitored on two of the electrodes by Elcor current integrators. High-frequency measurements (greater than 1 kHz) were made by using an oscilloscope across an appropriate load resistance from the electrode to ground. To reduce noise, coaxial cable was used for all electrode leads from outside the vacuum facility to the instruments.

The cylindrical configuration was mounted vertically in a horizontal, 3-meter-diameter, 5.2-meter-long vacuum tank. Figure 2 is a photograph of the inner cylinder as installed. The vacuum tank was pumped by six 32-inch, liquid-nitrogen-trapped, silicon-oil diffusion pumps.

THEORY

Theories on prebreakdown conduction across vacuum gaps usually invoke one of two mechanisms: field emission of electrons, or regenerative exchange of positive and negative ions. The first mechanism postulates either small dielectric inclusions giving rise to high local fields (and emission) or a macroscopic field causing the formation of whiskers on the metal cathode. The whiskers cause a local field intensification and resultant field emission from the whisker tips. The emission is given by the Fowler-Nordheim equation, which can be written approximately as

$$j \alpha E_\ell^2 \exp\left[-6.43\times10^9 \frac{\varphi^{3/2}}{E_\ell}\right] \tag{1}$$

where j is the current density in amperes per square meter, E_ℓ is the local field in volts per meter, and φ is the work function of the material in electron volts (ref. 12). For typical work functions it appears from equation (1) that a large increase in current occurs only as the local field approaches 10^{10} volts per meter. The local field can be given for a half ellipsoid of revolution on a flat plate by (ref. 7)

$$E_\ell = \beta E \tag{2a}$$

where

$$\beta = \frac{\lambda^2}{\ln \lambda} \tag{2b}$$

In these equations, E is the macroscopic field, β is the field intensification, and λ is the ratio of the semimajor axis of the ellipsoid to its semiminor axis (with this ratio assumed large).

The second mechanism postulates an organic contaminant coating on the electrodes of continuously pumped systems. This coating, according to reference 6, is a source of hydrogen ions, which, upon the application of a large enough voltage can be exchanged from cathode to anode and anode to cathode in a regenerative process. The requirement for current flow is

$$A(V) \cdot B(V) \geq 1 \tag{3}$$

where A, a function of applied voltage V, is the number of H^+ ions formed per impinging H^- ion, and B is the number of H^- ions formed per impinging H^+ ion. Measurements of A and B for unoutgassed surfaces find them approaching the condition of a contaminant coating (ref. 6).

RESULTS AND DISCUSSION

Threshold Voltage for Prebreakdown Current

A sharp threshold voltage for prebreakdown current was found at 44±4 kilovolts with positive polarity and at 50±0.4 kilovolts with negative polarity. (The polarity referred to is that of the inner cylinder with respect to ground.) In both cases, the electrodes were freshly cleaned and the pressure was in the range 10^{-7} to 10^{-8} torr. With the first voltage application, transient charging currents were observed that had time constants of about 1 second, which were in good agreement with a value of 1.3 seconds calculated from series resistance and capacitance values.

The time-averaged current at a constant voltage slightly below the threshold value was measured to be less than 0.01 microampere. At the threshold voltage, pulses of amplitude up to 500 microamperes with widths up to 100 millisecond began to occur. The form of a typical micropulse shown in figure 3 was similar to that found in reference 6. Pulses at threshold voltages became smaller in amplitude and longer in duration after the electrodes were conditioned. Pulses also exhibited this characteristic with the addition of a higher background gas pressure.

In this report, the threshold voltage is defined as the voltage required to initiate

recognizable micropulsing or to produce a time-averaged current of 1 microampere. The current flow at the threshold voltage was to the top end cap or to the outer cylinder. Current flow started to either one of these electrodes and then went to both at a slightly higher voltage. Current flow to the bottom end cap and to the negative junction shield was usually less than 1 microampere at all voltages since these electrodes were exposed to only a small area of the inner cylinder.

The occurrence of micropulsing with positive polarity at a macroscopic cathode field of 9×10^4 volts per meter requires a field intensification β of about 10^5 to produce a local field of 10^{10} volts per meter (see eq. (2a)). From equation (2b), because of this requirement λ for the conducting whiskers equals about 800. The fact that observed whiskers have λ's no larger than 10 (ref. 13) is a serious discrepancy with respect to that field emission model. The dielectric inclusion model is not amenable to direct evaluation from the experiment.

A nitrogen background gas had an extremely strong effect on the threshold voltage of freshly cleaned electrodes for both polarities. The situation for positive polarity is shown in figure 4, where the system threshold voltage is plotted as a function of nitrogen gas pressure. The threshold voltages are for the level region around 10^{-7} torr. An improvement by a factor of 12 or more results from a pressure of about 1×10^{-4} to 2×10^{-4} torr. At still higher pressures, the threshold voltage decreases again. The curve was repeatable, so apparently the pressure cycle had no progressive effect on the electrodes. Approximate calculations indicate that pressures of 1×10^{-4} to 2×10^{-4} torr are not large enough to cause significant energy losses for electrons traversing a gap. Therefore, provided the gamma ray environment would not reduce the effect, optimization of residual gas pressure might be a way to increase the operating voltage of a beta cell without conditioning.

No prebreakdown currents above 0.1 microampere were observed along the surface of the organic insulation under all experimental conditions tested. The threshold voltage for breakdown flashover along the surface was highly irregular from test to test. It was also observed that flashover might not occur up to 250 kilovolts during steady conditioning, but if the voltage were reduced to zero and several minutes were allowed to pass, flashover could occur at 150 kilovolts when the voltage would be raised again. The exact reason for this behavior is not known but may be related to variations in charge distribution on the surface of the insulator. Under most conditions, flashovers at a given voltage would stop after several breakdowns.

Characteristics of Gap Prebreakdown Currents

At the original threshold voltage (before conditioning) current flow consisted of

micropulses of frequency about 1 pulse per second (fig. 5(a)). As the voltage was increased above the threshold, the frequency of the micropulses increased while the amplitude decreased. As shown in figure 5(b), at 0.4 kilovolt above threshold, the frequency was 26 pulses per second and the amplitude was about 30 microamperes. As the voltage was increased further, a steady current occurred with the pulsing superimposed on the steady current. Figure 5(c) shows such a current at 13 kilovolts above threshold voltage. The steady current was about 20 microamperes, and the pulse frequency was about 50 pulses per second. Apparently the pulsing rate above the threshold voltage depends upon the difference between the applied and threshold voltages. As the difference gets larger, the pulses occur at a higher frequency. This is in agreement with what would be expected from simple resistance-capacitance circuit analysis. As the voltage is raised, the steady current becomes a larger fraction of the total time-averaged current. The appearance of a steady current is in agreement with the observations on prebreakdown currents for millimeter gaps in reference 5.

A plot of total time-averaged gap current against voltage above the instantaneous threshold voltage can be made for the prebreakdown conduction. In figure 6, these variables are plotted for two different original threshold voltages. The current increases to 50 microamperes with a 5- to 10-kilovolt voltage increase. For both cases, the slope decreases with increasing voltage. Insulator flashovers make it difficult to get more extensive curves of current against voltage above threshold.

When the voltage is raised above the original threshold to a given value and kept at that voltage for a period of time, the magnitude of current that is flowing slowly decreases. After several minutes of current flow at the constant voltage, a remeasurement of the threshold voltage shows that it has increased. The current can be returned to its former value only by applying a higher voltage. This phenomenon is called conditioning. Conditioning can be attributed to the elimination of the sharpest of the cathode whiskers according to the field-emission model, or to the reduction or modification of the contaminant coating according to the particle exchange model. With the exchange model, the restoration of the currents at higher voltages demands that the emission coefficients A and B increase with voltage. For outgassed surfaces, however, the coefficients decrease with increasing energy (ref. 14). This discrepancy in the theory has not been resolved as yet.

Prebreakdown Current Conditioning Rates

The voltage that produces a given time average gap current was found initially to increase linearly with the time that the given current flowed. This linear conditioning for high vacuum is shown in figure 7. A 20-microampere current produced a conditioning rate of 0.71 kilovolt per minute, and a 40-microampere current, a conditioning rate of

1.4 kilovolts per minute. Therefore, the voltage might be expected to increase linearly with the product of current and time, that is, with the charge. In figure 8, the total charge that has passed the inner and outer cylinders during a period of conditioning is plotted along the abscissa. The voltage that produces a 20-microampere current between the cylinders is plotted along the ordinate. A linear relation exists between these two variables. This is true for a time-averaged current range of 5 to 80 microamperes. Three different conditionings of a freshly cleaned configuration are shown. (The data in figs. 7 and 8(a) were taken with a lower voltage power supply and a 1.5×10^5-ohm surge-limiting resistance.)

The threshold voltage, previously defined as that voltage required to initiate micropulsing or produce a time-averaged current of 1 microampere, was also increased linearly with the total charge that passed between cylinders under some conditions. This is shown in figure 9. However, several limitations to the conditioning linearity were observed. For example, the initial nonlinearity shown in figure 9(b) is unexplained. Also, when the electrodes have been conditioned and time is allowed to pass so that reconditioning is necessary, the rate of increase of threshold voltage with charge was initially larger than the original rate. The upper limit of linearity was about 300 kilovolts with the inner cylinder positive (fig. 9(a)) and about 200 kilovolts with the inner cylinder negative (fig. 9(b)).

The results shown in figures 8 and 9(a) appear to be directly related as follows. An additional voltage above the threshold voltage must be applied to produce a given current, say, 20 microamperes. Figure 6 shows that this additional voltage is 3 kilovolts for a threshold voltage of 124 kilovolts and 2 kilovolts for a threshold voltage of 379 kilovolts. In either case, this additional voltage is small compared with the threshold voltage. Therefore, in conditioning, if the threshold voltage is linear with charge, the constant current voltage should also be approximately linear with charge.

Slopes for the conditioning process are quite reproducible and average about 1.0 kilovolt per millicoulomb for a solid outer cylinder. Variation from this mean for the three tests of figure 8 is less than 15 percent. From this conditioning rate, the time for a beta cell to reach 300 kilovolts can be calculated from

$$t = \frac{3.0}{i} \tag{4}$$

where t is the time in days, and i is the cell charging current in microamperes. With i equal to 0.1 microampere, t is 30 days, whereas, with i equal to 30 microamperes, t is 2.4 hours. The importance of an adequate current current supply for conditioning is apparent, particularly since the validity of equation (4) has not been demonstarted for long conditioning times. In fact, conditioning might not be expected to occur at all for small supplies of available current. The linear form for the voltage against charge

curves is felt to be general for vacuum gaps and not restricted to the cylindrical geometry.

Trends in conditioning rate dependence on various parameters can be determined from the data presented and from some preliminary studies with configurations not included in the APPARATUS section. For example, as shown in figure 9, the rate is approximately independent of polarity. For the same overall size and electric field, the rate decreased with increasing outer electrode area. This is seen by comparing figures 9(a) and 8. In the former case, the outer cylinder is a screen and the conditioning rate is 1.6 kilovolts per millicoulomb. In the latter case, the outer cylinder is solid with a larger surface area, and the conditioning rate is 1.0 kilovolt per millicoulomb. In a test involving a reduction in outer diameter and the same voltage (i.e., reduction in area and increase in field), the trend appeared to reverse. That is, in comparison to a rate of 1.0 kilovolt per millicoulomb with an 86-centimeter-diameter outer cylinder, the rate was 0.56 kilovolt per millicoulomb with a 61-centimeter-diameter outer cylinder. The conditioning rate thus seems to decrease with increasing electric field, although, additional tests may be indicated. Apparently, the reduction in area effect is more than offset by the increase in field. This may reflect the fact that, although the area varies directly with radius, the electric field varies inversely as the product of the radius and the logarithm of the radius.

The availability of hydrogen (through a layer of diffusion-pump oil applied to the inner cylinder with a damp cloth) also decreases the conditioning rate to about 0.5 kilovolt per millicoulomb for a 0.86-meter-diameter solid outer cylinder. These dependencies do not show a strong preference for either the field emission or the particle exchange model.

Vacuum Gap Limitations on Ultimate Voltage

Hard vacuum. - In the 10^{-7} to 10^{-8} torr range, the maximum voltage attainable in a given period of time was determined by the rate of conditioning of the electrodes. As indicated in figure 9, the threshold voltage starts to increase less than linearly with charge and appears to approach a limit asymptotically. From figure 9, extrapolated maximum threshold voltages were estimated to be about 390 kilovolts for positive polarity and about 330 kilovolts for negative polarity. With the inner cylinder positive, ultimate cathode and anode fields were 8.1×10^5 and 2.5×10^6 volts per meter, and with the inner cylinder negative, 2.1×10^6 and 6.9×10^5 volts per meter. Breakdowns occurred frequently during the conditioning. These produced complex responses on all meters for several microseconds, and conduction in the overload neon lamps. Visible sparks occurred along the insulator surface, but not across a vacuum gap.

Optimum background gas pressures. - With a nitrogen background gas pressure of 1×10^{-4} to 2×10^{-4} torr, the ultimate voltages were above the power-supply limit (600 kV).

Insulator Limitations on Ultimate Voltage

Occurrence of flashovers along the insulator surface did not appear to depend on gas pressure. A photograph of a 220-kilovolt breakdown with the pressure in the 10^{-7} torr range appears in figure 10. At higher pressures, there was more gas ionization, as shown in a breakdown at 2×10^{-4} torr, in figure 11. There was no effect on the insulator other than formation of a white haze on the surface. At higher voltages, breakdowns that were destructive to the insulator surface sometimes occurred. The negative junction shield was found to be very effective in reducing the occurrence of this type of breakdown.

For positive polarity, with little shielding, a polycarbonate insulator developed a surface leakage path along its entire length at 400 kilovolts after 225 breakdowns (fig. 12) and resistance was reduced to 200 megohms. Mechanically removing the conductive path by reducing the insulator diameter returned the insulation strength. With a concave shield (as in fig. 2), partial paths developed along the insulator surface to a point opposite the constriction of the shield in several tests. One of these is shown in figure 13. With the formation of these paths, the supported voltage was reduced to the range between 200 and 300 kilovolts. A plot of the equipotential lines in the vicinity of the insulator with the concave shield appears in figure 14. The plot was produced with the aid of a digital computer and the assumption of zero surface charge on the insulator. The plot shows an intense field between the insulator and the shield at the constriction. Breakdown currents apparently flowed along the insulator and jumped the vacuum gap at this high-field point. The currents were intense enough to produce insulator cracking. With a convex shield (as in fig. 1), however, breakdowns do not produce insulator cracking to the 600-kilovolt limit of the power supply.

For a beta-cell insulator (which has no electrical conductor passing through it as did the test configuration) the digital computer solution plotted in figure 15 indicates that the negative junction fields will be less severe than those tested (compare figs. 14 and 15). Also, insulator cracking would not be expected to occur for this case. Additional tests with the cable removed from the insulator, with negative polarity, and a concave trap at the inner cylinder end of the insulation produced no insulation cracking up to the 600 kilovolt limit.

TABLE I. - REDUCTION IN THRESHOLD VOLTAGE AS FUNCTION OF TIME AT ZERO APPLIED VOLTAGE WITH SYSTEM UNDER VACUUM

Threshold voltage at start of deconditioning, kV	Time of deconditioning, hr	Average threshold voltage reduction, kV
0 to 150	21	9
	66	27
150 to 300	0.80	36
	18	116
	65	134
300 to 450	18	143
	45	174

Voltage Deconditioning

The effects of high-voltage conditioning are not permanent (ref. 4), and with the present configuration, exposure to air with electrode handling and passage of time with the system under vacuum were observed to produce deconditioning. Reduction in threshold voltage with time for three ranges of original threshold voltage is shown in table I. The applied voltage was off during the test period. Scatter in individual data points was great. The average threshold voltage reduction, however, increases with time and tends to be greater with higher original threshold voltage.

CONCLUDING REMARKS

High-voltage measurements were made on a 30-centimeter-gap, concentric-cylinder electrode configuration in vacuum. The leakage current threshold voltage could be increased from 50 to 600 kilovolts by optimizing the residual nitrogen gas pressure level.

At high vacuum, and for a certain range of conditions, conditioned voltage was shown to be a function of the total charge that has passed across the gap between cylinders. Tests with polycarbonate materials indicated that a plain cylindrical insulator, 10.2 centimeters in diameter by 44.5 centimeters long, could withstand 600 kilovolts if properly shielded at the negative junction. The experimental results were not adequately explained by either the field-emission or the particle-exchange models of prebreakdown current.

National Aeronautics and Space Administration,
Lewis Research Center,
Cleveland, Ohio, December 28, 1966,
120-27-06-03-22.

REFERENCES

1. Low, Charles A., Jr.; and Mickelsen, William R.: An Electrostatic Propulsion System with a Direct Nuclear Electrogenerator. Aerospace Eng., vol. 21, no. 12, Dec. 1962, pp. 58-59, 72-87.

2. Cohen, Allan J.; and Low, Charles A., Jr.: A Parametric Study of Direct Nuclear Electrogenerator Cells Using a Beta Emitting Source. Paper No. 63048-B, AIAA, Mar. 11-13, 1963.

3. Plummer, A. M.; Gallagher, W. J.; Mathews, R. G.; and Anno, J. N.: The Alpha-cell Direct-Conversion Generator. Battelle Memorial Institute (NASA CR 54256), Nov. 30, 1964.

4. Arnal, Robert M.: Influence de la Concentration Superficielle d'hydrogène sur la Seuil des Macrodécharges Electriques dans le Vide. Compt. Rend., vol. 240, 1955, pp. 610-612.

5. Pivovar, L. I.; and Gordienko, V. I.: Micro-Discharges and Pre-Discharge Currents Between Metal Electrodes in High Vacuum. Soviet Phys. - Tech. Phys., vol. 3, no. 10, Oct. 1958, pp. 2101-2105.

6. Mansfield, W. K.; and Fortescue, R. L.: Pre-breakdown Conduction Between Electrodes in Continuously-Pumped Vacuum Systems. Brit. J. Appl. Phys., vol. 8, Feb. 1957, pp. 73-78.

7. Germain, C.; and Rohrbach, F.: Mechanism of Breakdown in a Vacuum. AEC-Tr-6341, 1963.

8. Gleichauf, Paul H.: Electrical Breakdown over Insulators in High Vacuum. J. Appl. Phys., vol. 22, no. 5, May 1951, pp. 535-541.

9. Kofoid, M. J.: Effect of Metal-Dielectric Junction Phenomena on High-Voltage Breakdown Over Insulators in Vacuum. AIEE Trans., Part III, Power Apparatus and Systems, vol. 79, Dec. 1960, pp. 999-1004.

10. Finke, Robert C.: A Study of Parameters Affecting the Maximum Voltage Capabilities of Shielded Negative Dielectric Junction Vacuum Insulators. Paper presented at the Second International Symposium on Insulation of High-Voltages in Vacuum, Cambridge, Mass., Sept. 7-9, 1966.

11. Koral, Kenneth F.: Prebreakdown Currents, High Voltage Configuration in Vacuum. Paper presented at the Second International Symposium on Insulation of High-Voltages in Vacuum, Cambridge, Mass., Sept. 7-9, 1966.

12. Charbonnier, F. M.: High Current Density Field Emission and the Transition to Vacuum Breakdown. Proceedings of the First International Symposium on the Insulation of High Voltages in Vacuum, Massachusetts Institute of Technology, 1964, pp. 23-24.

13. Little, R. P.; and Whitney, W. T.: Studies of the Initiation of Electrical Breakdown in Vacuum. Rep. No. 5944, Naval Research Lab., May 20, 1963.

14. Mitropon, I. M.; and Gumeniuk, V. S.: Emission of Negative Ions from Metallic Surfaces Bombarded with Positive Hydrogen Ions. Soviet Phys. - JETP, vol. 5, no. 2, Sept. 1957, pp. 157-164.

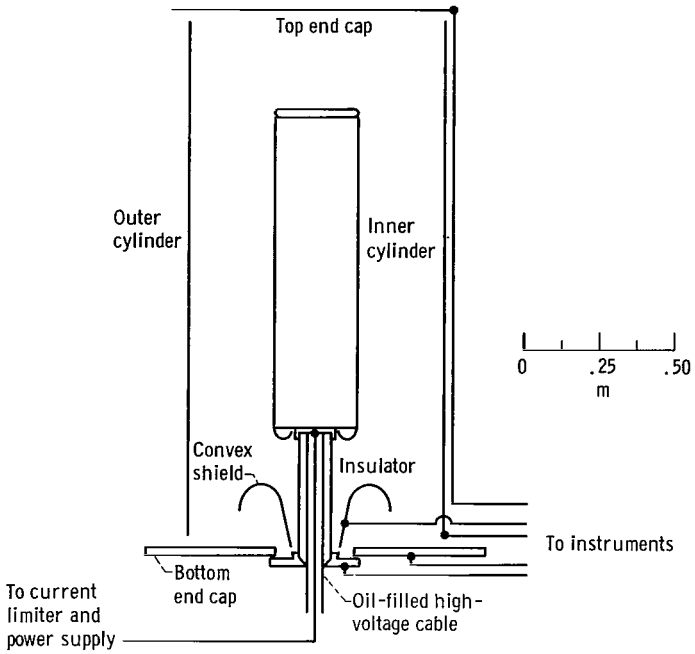

(a) Cross section of test configuration shown to scale.

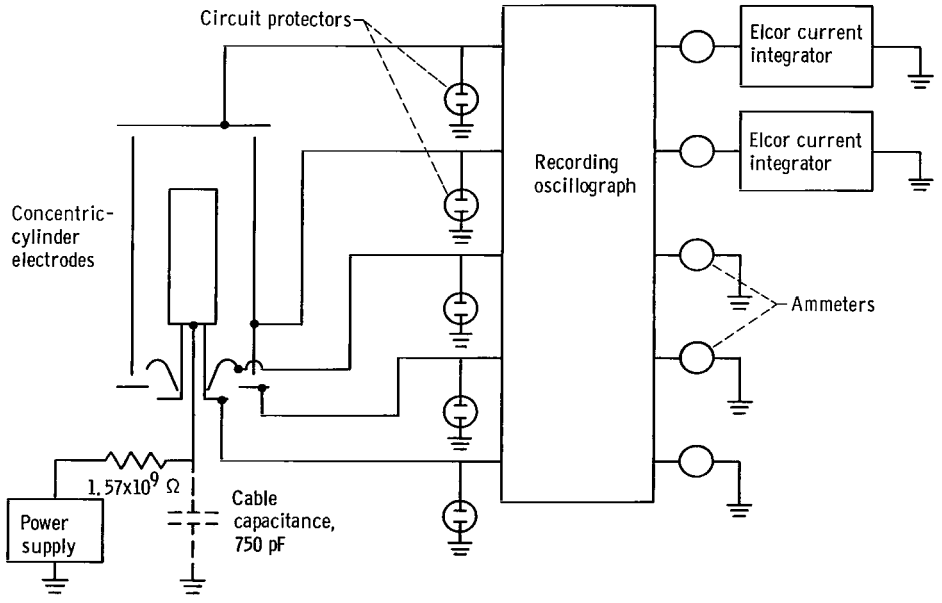

(b) Electrical connections for concentric cylinder test configuration.

Figure 1. - Test configuration.

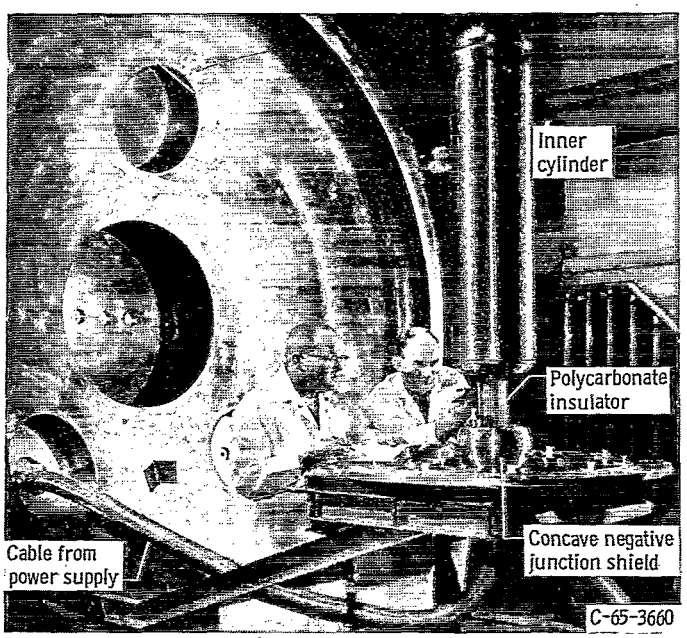

Figure 2. - Inner cylinder, feedthrough, and shield installed in position for test.

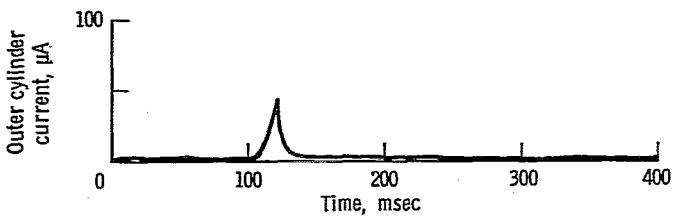

Figure 3. - Typical current micropulse at threshold voltage. Pressure, 1.2×10^{-7} torr; solid outer cylinder; positive polarity; average voltage, 88 kilovolts.

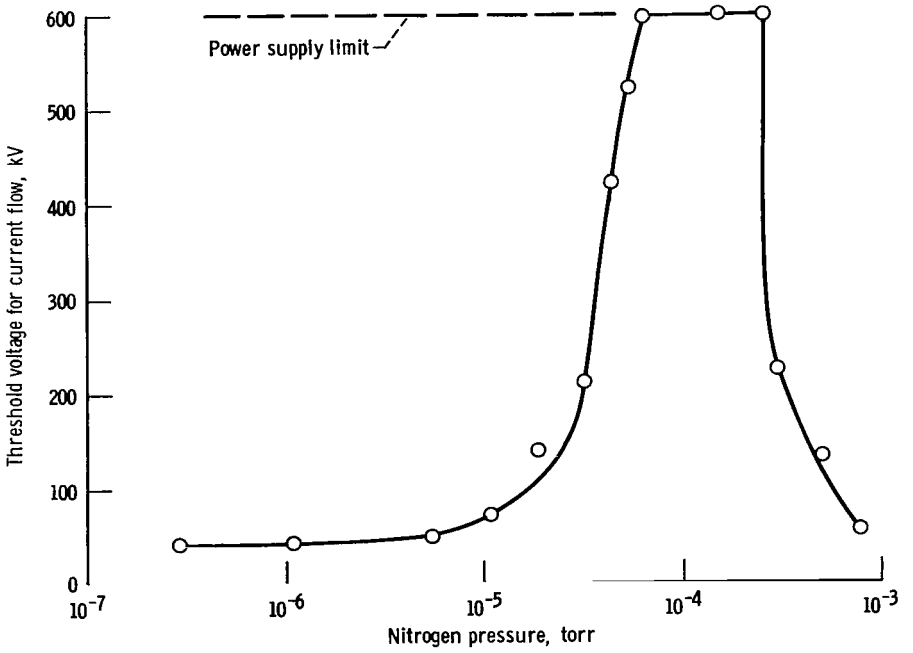

Figure 4. - Threshold voltage for unconditioned electrodes as function of nitrogen gas pressure. Screen outer cylinder.

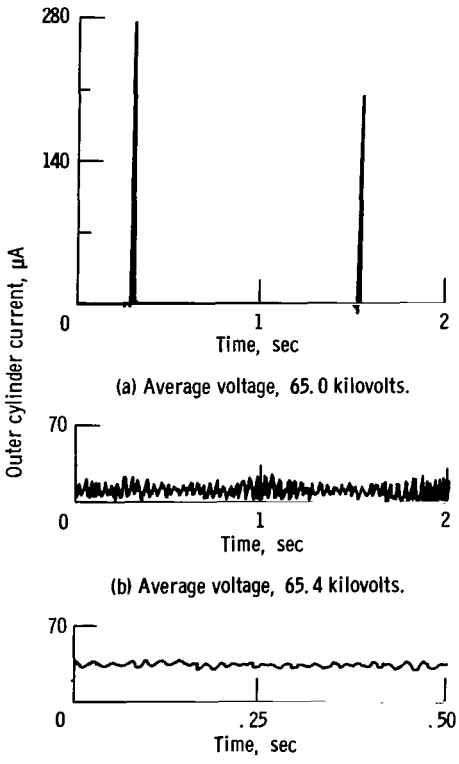

Figure 5. - Current characteristics as function of average voltage. Pressure, 5.0×10^{-7} torr; solid outer cylinder; positive polarity.

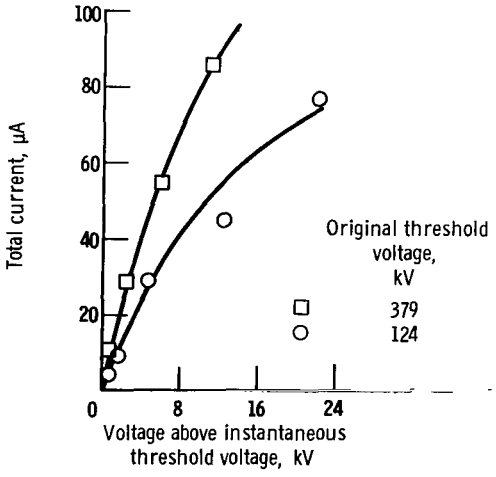

Figure 6. - Total of outer cylinder and top plate time-averaged gap current dependence on voltage. Pressure, 1.2×10^{-7} torr; solid outer cylinder; positive polarity.

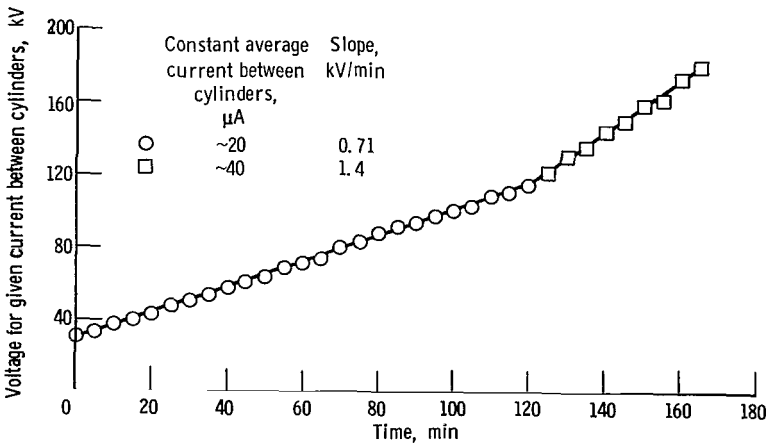

Figure 7. - Voltage as function of conditioning time at constant current. Pressure, 1.7×10^{-7} torr; solid outer cylinder; positive polarity.

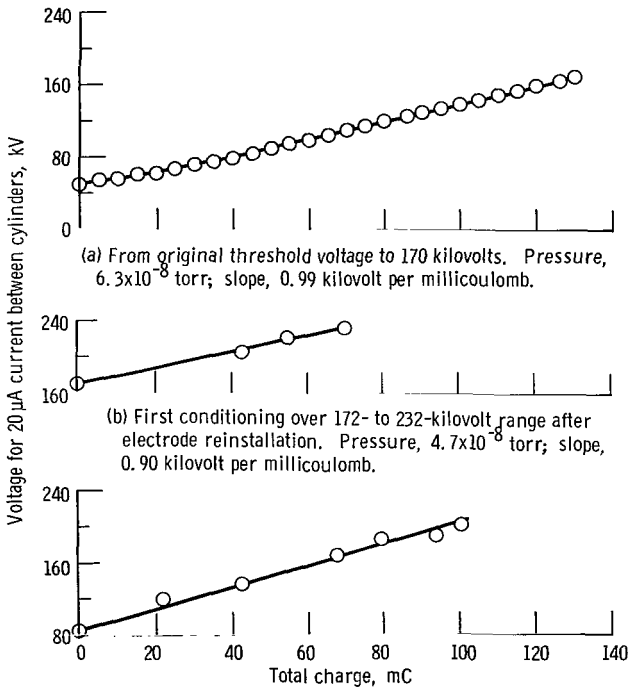

(a) From original threshold voltage to 170 kilovolts. Pressure, 6.3×10^{-8} torr; slope, 0.99 kilovolt per millicoulomb.

(b) First conditioning over 172- to 232-kilovolt range after electrode reinstallation. Pressure, 4.7×10^{-8} torr; slope, 0.90 kilovolt per millicoulomb.

(c) First conditioning over 85- to 200-kilovolt range after electrode reinstallation. Pressure, 1.0×10^{-7} torr; slope, 1.14 kilovolts per millicoulomb.

Figure 8. - Voltage as function of total charge transferred between cylinders for three tests with freshly cleaned electrodes. Solid outer cylinder; positive polarity.

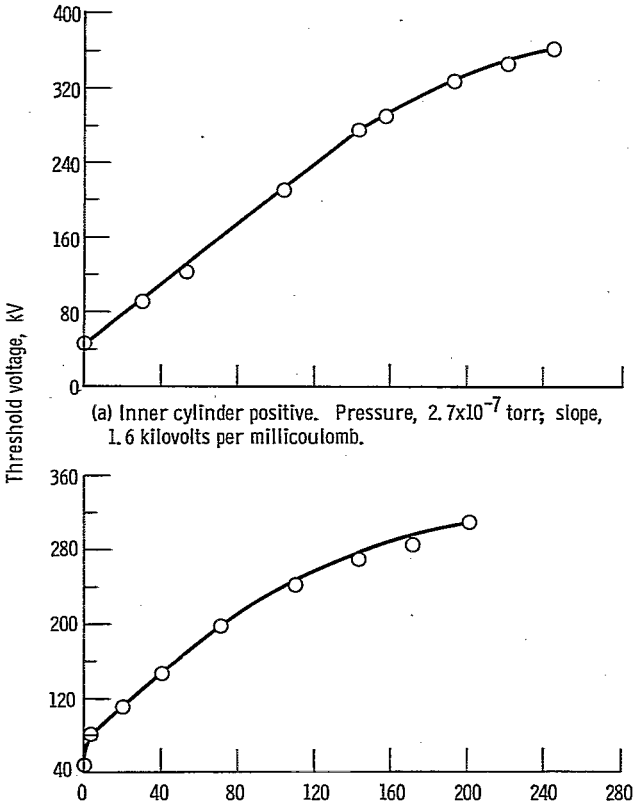

(a) Inner cylinder positive. Pressure, 2.7×10^{-7} torr; slope, 1.6 kilovolts per millicoulomb.

(b) Inner cylinder negative. Pressure, 6.8×10^{-7} torr; slope, 1.7 kilovolts per millicoulomb.

Figure 9. - Threshold voltage as function of total charge with freshly cleaned electrodes. Screen outer cylinder.

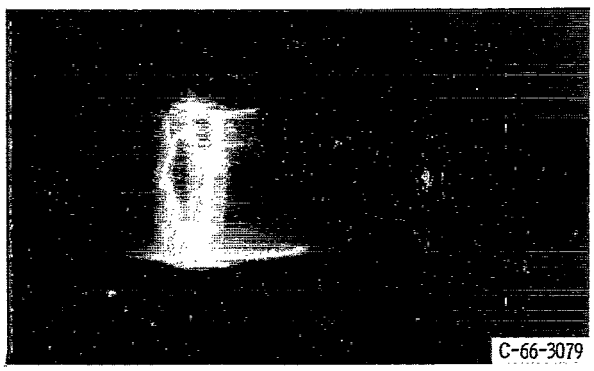

Figure 10. - Spark breakdown over surface of polycarbonate insulator at 220 kilovolts. Polarity is positive, outer cylinder is a screen, and negative junction shield is convex.

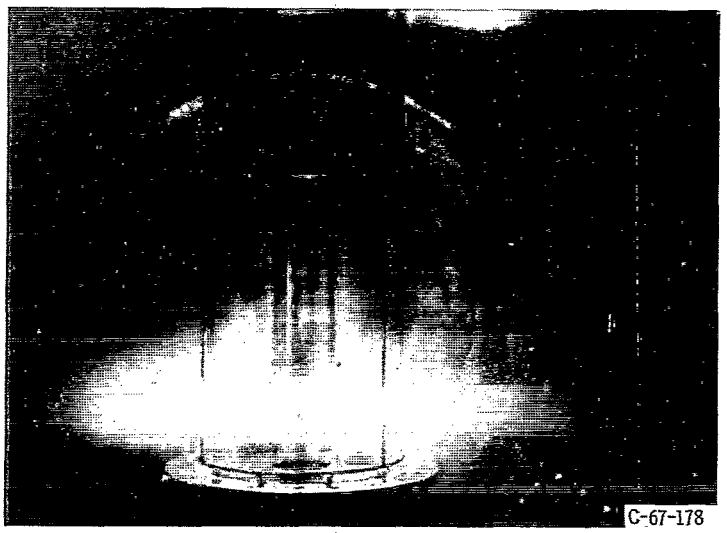

Figure 11. - Spark breakdown at 2×10^{-4} torr. (Photograph made with 3000 ASA speed film and time exposure.)

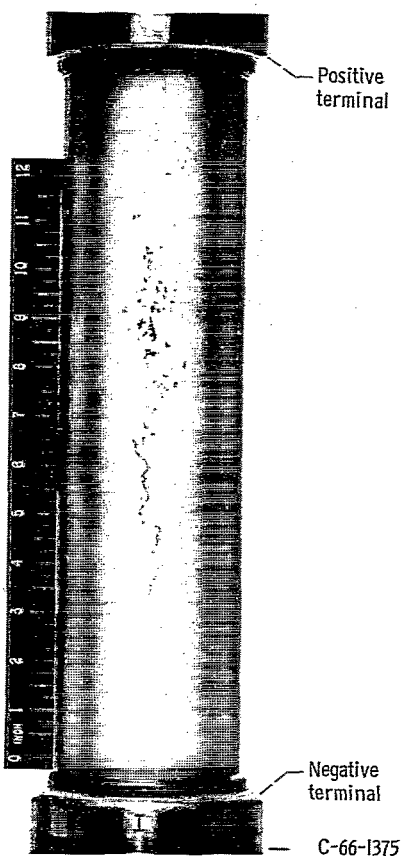

Figure 12. - Polycarbonate insulator after test with little negative junction shielding. Conduction path curves around cylinder at negative end.

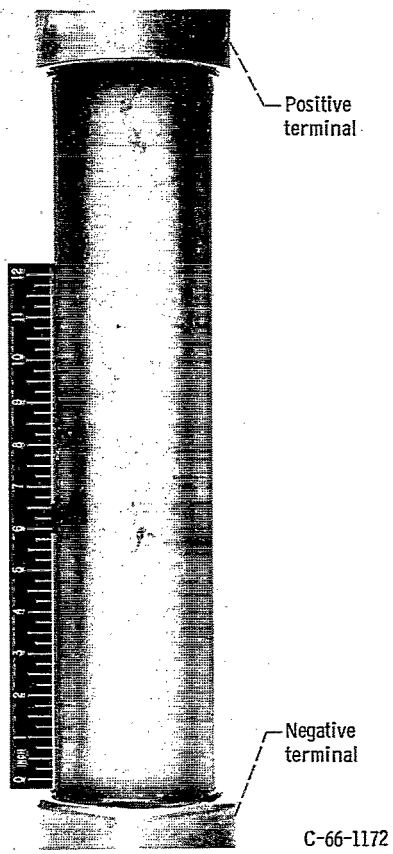

Figure 13. - Polycarbonate insulator after test with concave shield. Top of shield located at 6 1/4 inch mark; cracking on surface only.

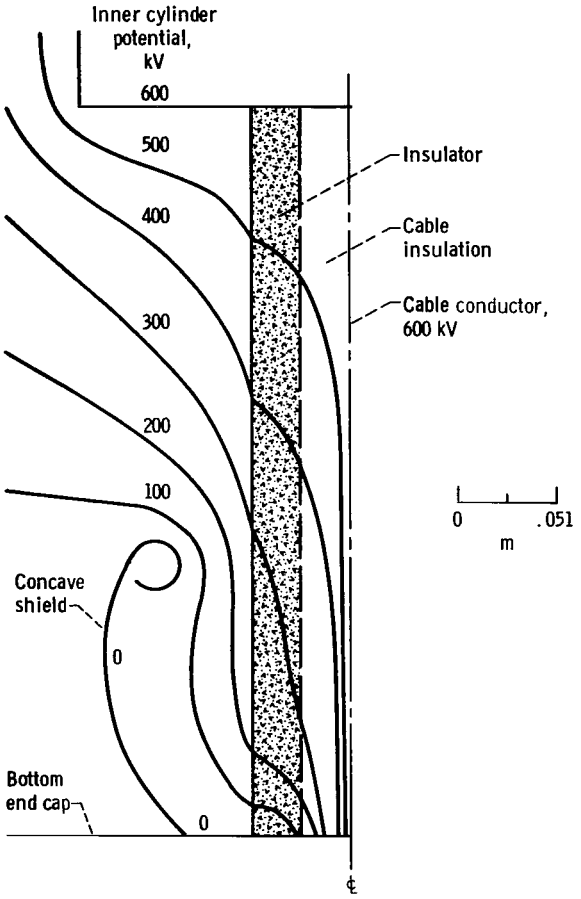

Figure 14. - Equipotential lines for insulator annulus and cable with concave shield. Inner cylinder at 600 kilovolts.

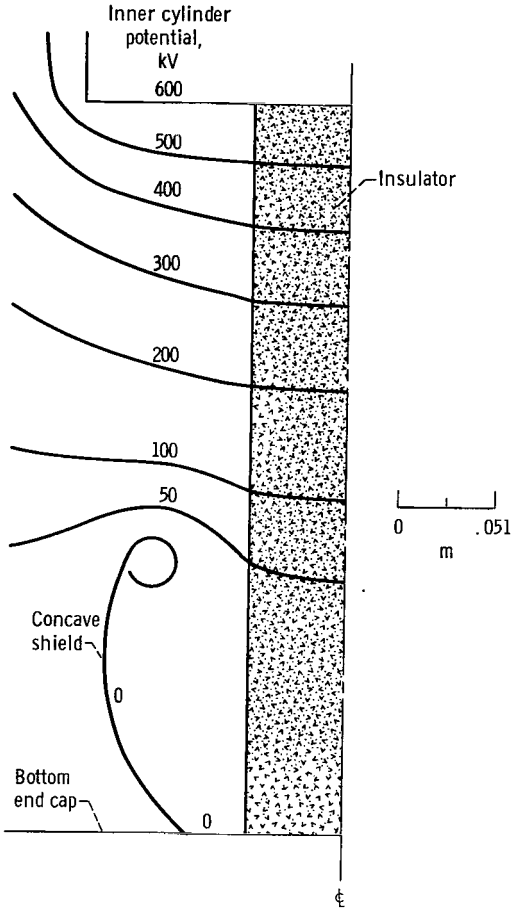

Figure 15. - Equipotential lines for 0.44-meter-long, 0.102-meter-diameter insulator. Inner cylinder at 600 kilovolts.

NASA-Langley, 1967 —— 28 E-3635

"The aeronautical and space activities of the United States shall be conducted so as to contribute . . . to the expansion of human knowledge of phenomena in the atmosphere and space. The Administration shall provide for the widest practicable and appropriate dissemination of information concerning its activities and the results thereof."

—NATIONAL AERONAUTICS AND SPACE ACT OF 1958

NASA SCIENTIFIC AND TECHNICAL PUBLICATIONS

TECHNICAL REPORTS: Scientific and technical information considered important, complete, and a lasting contribution to existing knowledge.

TECHNICAL NOTES: Information less broad in scope but nevertheless of importance as a contribution to existing knowledge.

TECHNICAL MEMORANDUMS: Information receiving limited distribution because of preliminary data, security classification, or other reasons.

CONTRACTOR REPORTS: Scientific and technical information generated under a NASA contract or grant and considered an important contribution to existing knowledge.

TECHNICAL TRANSLATIONS: Information published in a foreign language considered to merit NASA distribution in English.

SPECIAL PUBLICATIONS: Information derived from or of value to NASA activities. Publications include conference proceedings, monographs, data compilations, handbooks, sourcebooks, and special bibliographies.

TECHNOLOGY UTILIZATION PUBLICATIONS: Information on technology used by NASA that may be of particular interest in commercial and other non-aerospace applications. Publications include Tech Briefs, Technology Utilization Reports and Notes, and Technology Surveys.

Details on the availability of these publications may be obtained from:

SCIENTIFIC AND TECHNICAL INFORMATION DIVISION

NATIONAL AERONAUTICS AND SPACE ADMINISTRATION

Washington, D.C. 20546